Anti-Lock Brake System Control for Buses Based on Fuzzy Logic and a Sliding-Mode Observer

Jong Hyeon Park*, Dong Hee Kim, Yong Ju Kim
School of Mechanical Engineering, Hanyang University, Seoul 133-791, Korea

In this paper, an anti-lock brake system (ABS) for commercial buses is proposed based on a fuzzy-logic controller and a sliding-mode observer of the vehicle speed. The brake controller generates pulse width modulated (PWM) control inputs to the solenoid valve of each brake, as a function of the estimated wheel slip ratio. PWM control inputs at the brakes significantly reduce chattering in the brake system compared with conventional on-off control inputs. The sliding-mode observer estimates the vehicle speed with measurements of wheel speed, which is then used to compute the wheel slip ratio. The effectiveness of the proposed control algorithm is validated by a series of computer simulations of bus driving, where the 14-DOF bus model is used.

Key Words : ABS, Commercial Bus, Fuzzy Logic, Sliding-Mode Observer

Nomenclature

A_f : Frontal cross-sectional area of the vehicle
A_s : Side cross-sectional area of the vehicle
C_a : Cornering stiffness of a tire
C_i : Longitudinal stiffness of a tire
C_{df} : Frontal drag coefficient
C_{ds} : Side drag coefficient
D_x : Longitudinal drag force
D_y : Lateral drag force
F_{ri} : Rolling resistance of tire i
F_{si} : Suspension force generated at suspension i
F_{xi} : Tractive force generated by tire i
F_{yi} : Lateral force generated by tire i
I_x : Roll inertia of the sprung mass
I_y : Pitch inertia of the sprung mass
I_z : Yaw inertia of the sprung mass
I_{wi} : Inertia moment of a wheel i
I_{uf} : Front axle inertia moment
I_{ur} : Rear axle inertia moment
K_t : Vertical stiffness of a tire
K_{rf} : Roll stiffness of the front axle
K_{rr} : Roll stiffness of the rear axle
M : Mass of the vehicle
M_{zi} : Self aligning torque at tire i
R : Radius of tires
T_{bi} : Brake torque applied at tire i
T_{si} : Engine torque applied at tire i
V_x : Longitudinal speed of the vehicle
V_y : Lateral speed of the vehicle
e : Distance between the roll center and the center of gravity
h : Height of the center of gravity above the ground
i : Wheel or tire index, $i=\{1, 2, 3, 4\}$ or $\{f, r\}$
l_f : Distance between the front axle and the center of gravity
l_r : Distance between the rear axle and the center of gravity
m : Total mass of the vehicle
m_s : Sprung mass
m_u : Unsprung mass
t_f : Front tread
t_r : Rear tread
δ_i : Steering angle of tire i
λ : Slip ratio of a tire
μ : Friction coefficient
ω_f : Speed of front wheel

* Corresponding Author,
E-mail : jongpark@hanyang.ac.kr
TEL : +82-2-2290-0435; **FAX** : +82-2-2298-4634
School of Mechanical Engineering, Hanyang University, Seoul 133-791, Korea (Manuscript **Received** February 13, 2001; **Revised** August 3, 2001)

ω_r : Speed of rear wheel
ρ : Density of air
ε_r : Road adhesion reduction factor

1. Introduction

With a rapid progress of automotive industry in recent years, there has been an increasing need for a vehicle safety, more specifically, vehicle stability, maneuverability, and enhancement in braking performance. Especially, active safety systems such as ABS(Anti-lock Brake System), TCS (Traction Control System), 4WS (4-Wheel Steering) and yaw moment control have been studied by many researchers. While these systems are employed in many passenger cars, only a limited number of commercial vehicles are equipped with such systems. However, since commercial inter-state buses take a large number of people on board, more attention should be paid to their safety.(Kawabe et al., 1997 : Hattori et al., 1998 : Akey, 1995 ; Raza, 1997 ; Zanten et al., 1996 ; Choi and Cho, 1998)

For ABS controls, many researches have been conducted. Some of the examples are PID control, sliding-mode control, fuzzy control, and discrete time control [1, 2, 3, 4, 5, 7]. In many advanced ABS controls, it is necessary to compute the slip ratio of the vehicle in order for the controller to keep the slip ratio of the vehicle at a certain target value. This in turn requires measurements of vehicle speed. However, it is difficult to measure the vehicle speed accurately, and directly from sensors, while the wheel angular velocity can be directly measured with wheel-speed sensors. Two of the many methods to measure the vehicle velocity are to use magnetic markers imbedded in the pavement and to use an accelerometer to compute vehicle velocity by integration. However, both methods have drawbacks: one requires an accurate sensing system and infrastructure, the other is frequent updates because of accumulation of integration errors (Unsal and Kachroo, 1999). Thus, it is practically necessary to have an estimator of vehicle speed.

Due to the intrinsic nonlinearity of vehicle dynamics, nonlinear observers such as sliding -mode observers, extended Kalman filters and their variations, for example, a rule-based Kalman filter (Watanabe and Kobayashi, 1989), a combination of a nonlinear sliding-mode observer and an extended Kalman filter (Unsal and Kachroo, 1999), and fuzzy-logic estimators (Zimmer, 1996) have been proposed. While the performance of extended Kalman filters could be degraded by modelling errors, sliding mode observers potentially offer advantages in its inherent robustness to parametric uncertainties. Furthermore, contrary to sliding-mode controllers, chattering in sliding-mode observers is only a numerical issue rather than mechanical limitations to overcome (Slotine et al., 1987).

In this paper, we propose a fuzzy-logic controller for ABS systems based on the estimation of the wheel slip ratio with a sliding-mode observer. Fuzzy-logic is employed to minimize the effort of tuning control parameters and to deal with nonlinear vehicle dynamics. The proposed ABS controller generates pulse-width-modulated (PWM) signals and regulates the pressure variation more accurately than the conventional controllers which generate on-off signals.

We also propose a sliding-mode observer to estimate the vehicle speed from the measured wheel angular velocity. Unlike the work by Unsal and Kachroo (Unsal and Kachroo, 1999), where the gains were found by trial-and-error, the gains of the estimator are selected such that the error in thevehicle speed mathematically converges to zero, based on the vehicle dynamics and the tire characteristics of Dugoff's model.

The verification of the sliding-mode observer and the fuzzy-logic controller are conducted in computer simulations of driving a nonlinear 14 -DOF vehicle model.

2. Vehicle Model

2.1 Vehicle dynamics

In this paper, the bus dynamics is modelled as a nonlinear 14-DOF system shown in Fig. 1 which is used in the later simulations of vehicle driving under different conditions. It is assumed

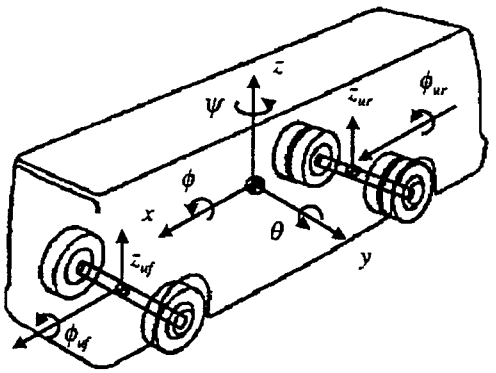

Fig. 1 A nonlinear 14-DOF vehicle model

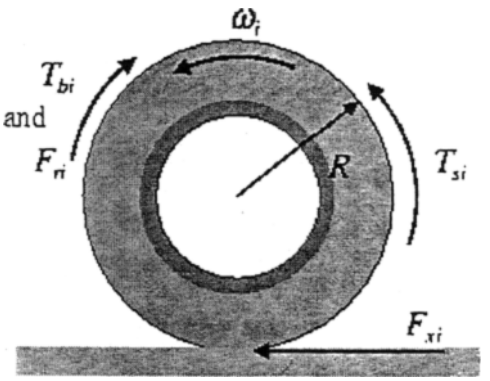

Fig. 2 A model of forces applied at a wheel

that a bus consists of 7 main parts: the sprung mass, front and rear unsprung masses, and four wheels.

The dynamic equations of the vehicle in the longitudinal, lateral, vertical, rolling, pitching, and yawing directions are as follows:

$$m\ddot{x}+m_s e\ddot{\theta}=\sum_{i=1}^{4} T_{xi}-D_x-m(\dot{z}\dot{\theta}-\dot{y}\dot{\psi})$$
$$-m_s e\dot{\phi}\dot{\psi}+(m_{uf}l_f-m_{ur}l_r)\dot{\psi}^2 \quad (1)$$
$$m\ddot{y}-m_s e\ddot{\phi}+(m_{uf}l_f-m_{ur}l_r)\ddot{\psi}$$
$$=\sum_{i=1}^{4} T_{yi}-D_y-m(\dot{x}\dot{\psi}-\dot{z}\dot{\phi})-m_s e\dot{\theta}\dot{\psi} \quad (2)$$
$$m_s\ddot{z}=\sum F_{si}-m_s(-\dot{x}\dot{\theta}-\dot{y}\dot{\phi}-e\dot{\phi}^2-e\dot{\theta}^2) \quad (3)$$
$$-m_s e\ddot{y}+(I_x+m_s e^2)\ddot{\phi}=(I_y-I_z)\dot{\phi}\dot{\psi}$$
$$+b\sum_{i=1}^{4} T_{yi}-t_f(F_{s1}-F_{s2})-t_r(F_{s3}-F_{s4})$$
$$+m_s ge\sin\phi+m_s e(\dot{x}\dot{\psi}-\dot{z}\dot{\phi}+e\dot{\theta}\dot{\psi})$$
$$-(K_{rf}+K_{rr})\phi+K_{rf}\phi_{uf}+K_{rr}\phi_{ur} \quad (4)$$
$$I_y\ddot{\theta}=(I_z-I_x)\dot{\phi}\dot{\psi}-h\sum_{i=1}^{4} T_{xi}$$
$$+l_f(F_{s1}+F_{s2})-l_r(F_{s3}+F_{s4}) \quad (5)$$
$$I_z\ddot{\psi}=(I_x-I_y)\dot{\phi}\dot{\theta}+l_f(T_{y1}+T_{y2})$$
$$-l_r(T_{y3}+T_{y4})-t_f(T_{x1}-T_{x2})$$
$$-t_r(T_{x3}-T_{x4})-\sum_{i=1}^{4} M_{zi} \quad (6)$$

where

$$T_{xi}=F_{xi}\cos\delta_i-F_{yi}\sin\delta_i$$
$$T_{yi}=F_{xi}\sin\delta_i+F_{yi}\cos\delta_i$$
$$D_x=\frac{1}{2}\rho A_f C_{df} V_x^2$$
$$D_y=\frac{1}{2}\rho A_s C_{ds} V_y^2$$

The dynamic equations of the unsprung mass are as follows: Equations (7) and (8) represent translation motions in the vertical direction, and Eqs. (9) and (10) represent rotation motions in the rolling direction.

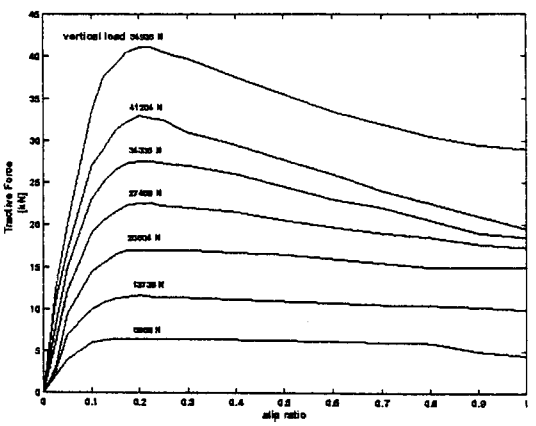

Fig. 3 Tractive force of the tire used in the simulation

$$m_{uf}\ddot{z}_{uf}=F_{s1}+F_{s2}-K_t(z_{uf}-z_{r1}+t_f\phi_{uf})$$
$$-K_t(z_{uf}-z_{r2}-t_f\phi_{uf}) \quad (7)$$
$$m_{ur}\ddot{z}_{ur}=F_{s3}+F_{s4}-2K_t(z_{ur}-z_{r3}+t_r\phi_{ur})$$
$$-2K_t(z_{ur}-z_{r4}-t_r\phi_{ur}) \quad (8)$$
$$I_{uf}\ddot{\phi}_{uf}=t_fF_{s1}-t_fF_{s2}-t_fF_{t1}$$
$$+t_sF_{t2}-K_{rf}(\phi_{uf}-\phi) \quad (9)$$
$$I_{ur}\ddot{\phi}_{ur}=t_rF_{s3}-t_rF_{s4}-t_rF_{t3}$$
$$+t_rF_{t4}-K_{rr}(\phi_{ur}-\phi) \quad (10)$$

For driving the i-th wheel, its governing dynamics can be derived from Fig. 2 as

$$I_{wi}\dot{w}_i=T_{si}-T_{bi}-R\cdot F_{xi}-F_{ri} \quad (i=1, 2, 3, 4) \quad (11)$$

In braking and cornering, vehicle characteristics depend on the tire forces. In vehicle dynamics studies, a good representation of tire behavior is important to describe the vehicle

motion. Due to the lack of data on bus tires, we developed a discrete model of the truck tire 295/75R22.5 based on experimental data (Kurke et al., 1989). The relationship between the tractive force and the slip ratio in the model is shown in Fig. 3.

2.2 Brake model

While hydraulic brake systems are used in passenger cars, commercial vehicles such as buses are equipped with air brake systems. Air brake systems are more sluggish than hydraulic systems due to the compressibility of air. A typical air-brake system basically consists of brake valves, a pressure control valve (PCV), and wheel cylinders. We modelled the air-brake system as a 1st-order plant with a pure time delay (Choi and Cho, 1998), which reflects the sluggishness due to the air compressibility.

$$\dot{p}(t)=-\frac{p(t)}{\tau}u_1(t-T)+\frac{P_d(t)-p(t)}{\tau}(1-u_2(t-T)) \quad (12)$$

where $p_d(t)$ is the pressure applied by a driver; $p(t)$ is the pressure at the wheel cylinder; T and τ denote the time delay and the time constant of air brake system, respectively; u_1 is the control input for the outlet valve and u_2 is the control input to the pressure-holding valve. For less sophisticated PCV, simpler control inputs of binary signal are used, i. e., either 0 or 1 is used as input signals. Control inputs to the valves used in the work are PWM (pulse-width-modulation) signals, which can be any number between 0 and 1 depending on the duty rate. The PCV operates in 3-stages: pressure build-up, pressure hold, and pressure release. When $u_1=0$ and $0<u_2<1$, the pressure increases and the increasing speed is proportional to the magnitude of u_2. When $0<u_1<1$ and $u_2=0$, the pressure decreases and the decreasing speed is proportional the magnitude of u_1. When the pressure is to be maintained at a constant level, the value control inputs of $u_1=0$ and $u_2=1$ are issued.

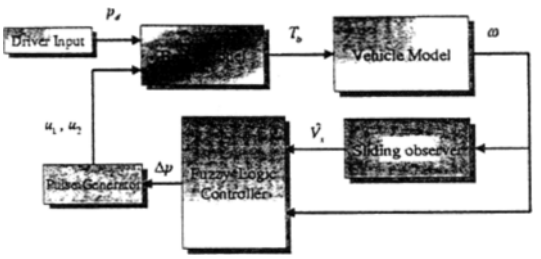

Fig. 4 The overall system block diagram

3. Fuzzy-Logic Controller

Because fuzzy-logic controllers can deal with inaccuracy in a rigorous manner, they are effective at handling the uncertainties and nonlinearities associated with complex systems (Lin and Lee, 1996). The fuzzy-logic controller proposed here regulates the wheel slip by controlling the brake pressure of each wheel. The control objective is to maintain the slip ratio of each wheel approximately at 0.2. Figure 4 shows the overall system block-diagram including the vehicle speed observer.

We choose the slip ratio, λ, and the wheel acceleration, a_ω, as control variables. They are computed based on the vehicle speed and the wheel angular speed:

$$\lambda=\frac{V_x-R\cdot\omega}{V_x},\ a_\omega=\frac{\omega(t)-\omega(t-T)}{\Delta t}. \quad (13)$$

Each of the fuzzy inputs of wheel acceleration (WA) and slip ratio (SR) is expressed by 5 fuzzy-membership functions: "Very Low" (VL), "Low" (L), "Medium" (M), "High"(H), and "Very High" (VH). The output of the fuzzy-logic controller is the desired pressure differential, Δp, and is expressed by 5 fuzzy-membership functions: "High Pressure Decrease" (HPD), "Low Pressure Decrease" (LPD), "Holding Pressure" (HP), "Low Pressure Increase" (LPI), and "High Pressure Increase" (HPI). Fuzzy-membership functions for the inputs and output are shown in Fig. 5.

Fuzzy rules used here are based on conventional ABS algorithms. A typical conventional ABS algorithm works as follows: When the wheel acceleration decreases beyond a certain

Table 1 Fuzzy rule-base

Slip Ratio (λ)	Wheel Acceleration (a_ω)				
	VLWA	LWA	MWA	HWA	VHWA
VLSR	HPI	HPI	HPI	HPI	HPI
LSR	HP	HP	LPI	HP	HPI
MSR	HP	HP	LPI	HP	HPI
HSR	HPD	HPD	LPD	LPI	HPI
VHSR	HPD	HPD	HPI	HPD	HPI

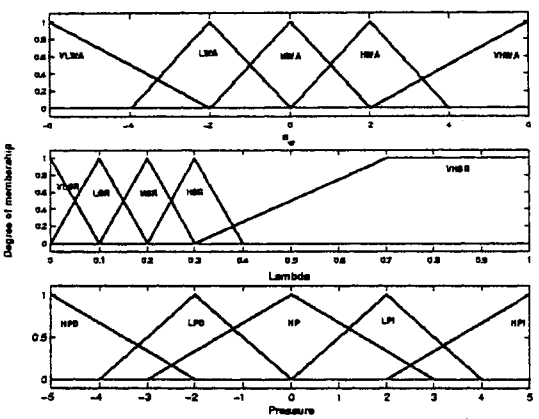

Fig. 5 Membership functions of inputs and output

threshold value $(-a)$ due to braking, the solenoid valve is shifted to its "maintain pressure" position. When the wheel peripheral velocity drops further below a slip ratio threshold, the solenoid valve is shifted to its "pressure release" position. The brake pressure then continues to drop until the wheel's peripheral acceleration exceeds again threshold $(-a)$ again. Then, the solenoid valve is shifted to hold the brake pressure. When the wheel's acceleration increases and exceeds a threshold $(+a)$, the solenoid value is shifted to increase the brake pressure.

A fuzzy-logic ABS controller is designed to behave similar to conventional ABS controllers, and its logic is summarized in Table 1. The fuzzy inference used is based on Mamdani's method and defuzzification is based on the centroid of area method.

The output from the fuzzy-logic controller is transformed to the PWM inputs to the pressure control value by the pulse generator according to its working principle explained in subsection 2.2. Thus,

$$\begin{cases} u_1=0,\ u_2=\Delta p/p_0, & \text{when } \Delta p>\varepsilon p_0 \\ u_1=-\Delta p/p_0,\ u_2=0, & \text{when } \Delta p<-\varepsilon p_0, \\ u_1=0,\ u_2=1, & \text{when } |\Delta p|\le\varepsilon p_0 \end{cases} \quad (14)$$

where p_0 is the maximum pressure and ε is a small positive constant.

4. Sliding-Mode Observer

In practical applications for ABS, vehicle speed cannot be measured reliably with sensors only. In this paper, a sliding-mode observer is designed to estimate vehicle speed with the measurement of the wheel angular speed and the vehicle dynamic model. For the observer, only a simplified vehicle model is considered here. Thus, a 3-DOF vehicle model is developed. This model allows vehicle motions in the forward direction and the front and rear wheel rotations.

$$\dot{x}=f(x,\ t)=\begin{bmatrix} (F_{xf}+F_{xr})/M \\ (-T_{bf}-R\cdot F_{xf}-rr_f)/I_{\omega f} \\ (-T_{br}-R\cdot F_{xr}-rr_r)/I_{\omega r} \end{bmatrix} \quad (15)$$

where $x=[V_x\ \omega_f\ \omega_r]^T$; subscript f and r denote the front and rear wheel, respectively.

Suppose that only the wheel angular velocities are available as the output, and thus,

$$y=\begin{bmatrix}\omega_f \\ \omega_r\end{bmatrix}=Cx=\begin{bmatrix}0&1&0\\0&0&1\end{bmatrix}x. \quad (16)$$

The sliding-mode observer is represented by

$$\dot{\hat{x}}=\hat{f}(\hat{x},\ t)-H\tilde{y}-K\mathrm{sgn}(\tilde{y}) \quad (17)$$

where $\hat{f}(\hat{x},\ t)$ is simplified 3-DOF model of actual plant $f(x,\ t)$. $H,\ K\in\Re^{3\times2}$ are linear and nonlinear gain matrices to be selected, and estimation error on the output is defined such as

$$\tilde{y}:=\hat{y}-y=C\hat{x}-Cx \quad (18)$$

and

$$\mathrm{sgn}(\tilde{y})=\begin{bmatrix}\mathrm{sgn}(\tilde{y}_1)\\ \mathrm{sgn}(\tilde{y}_2)\end{bmatrix}.$$

From Eqs. (15) and (17), the error dynamics becomes

$$\dot{\tilde{x}}=\Delta f(\tilde{x},\ t)-H\tilde{y}-K\mathrm{sgn}(\tilde{y}) \quad (19)$$

where

$$\Delta f(\tilde{x}, t) = \hat{f}(\hat{x}, t) - f(x, t). \tag{20}$$

We also define the sliding surface as

$$s := \tilde{y} = C(\hat{x} - x). \tag{21}$$

Consider a Lyapunov function candidate as

$$V = \frac{1}{2} s^T s. \tag{22}$$

Differentiating it,

$$\begin{aligned}\frac{1}{2}\frac{d}{dt}(s^T s) &= s^T \dot{s} = \tilde{y}^T \dot{\tilde{y}} = \tilde{y}^T C \dot{\tilde{x}} \\ &= \tilde{y}^T C(\Delta f - H\tilde{y} - K\mathrm{sgn}(\tilde{y})) \\ &= -\tilde{y}^T C H \tilde{y} + \tilde{y}^T C(\Delta f - K\mathrm{sgn}(\tilde{y})).\end{aligned} \tag{23}$$

If H is selected such that

$$H = \begin{bmatrix} h_{11} & h_{12} \\ 1 & 0 \\ 0 & 1 \end{bmatrix} \tag{24}$$

then $\tilde{y}^T C H \tilde{y} \geq 0$, and

$$\begin{aligned}&\tilde{y}^T C(\Delta f - K\mathrm{sgn}(\tilde{y})) \\ &= \tilde{y}_1(\Delta f_2 - k_{21}\mathrm{sgn}(\tilde{y}_1) - k_{22}\mathrm{sgn}(\tilde{y}_2)) \\ &+ \tilde{y}_2(\Delta f_3 - k_{31}\mathrm{sgn}(\tilde{y}_1) - k_{32}\mathrm{sgn}(\tilde{y}_2)).\end{aligned} \tag{25}$$

In order to avoid couplings between variable $\tilde{y}_1$ and $\tilde{y}_2$ in Eq. (25), we let

$$k_{22} = k_{31} = 0. \tag{26}$$

Moreover, if k_{21} and k_{32} are selected such that

$$k_{21} > |\Delta f_2| + \eta_1, \quad k_{32} > |\Delta f_3| + \eta_2 \tag{27}$$

where η_1 and η_2 are positive constants, sliding condition in Eq. (23) is as follows:

$$\frac{1}{2}\frac{d}{dt}(s^T s) \leq -\eta_1 |\tilde{y}_1| - \eta_2 |\tilde{y}_2| < 0. \tag{28}$$

Since the sliding conditions are satisfied, $\tilde{y}$ converges to zero. Now, the other gains should be selected such that the error in the vehicle longitudinal velocity, $\tilde{x}_1$ also converges to zero.

On the sliding surface, the system satisfies the condition $s = \dot{s} = 0$. Hence, the dynamics of the system on the sliding surface can be derived using these conditions (slotine et al., 1987 : Misawa and Hedrick, 1989). Using Eqs. (17) and (21),

$$\dot{s} = C\dot{\tilde{x}} = C(\Delta f - K\mathrm{sgn}(\tilde{y})) = 0 \tag{29}$$

or

$$CK\mathrm{sgn}(\tilde{y}) = C\Delta f. \tag{30}$$

Substituting Eq. (30) into Eq. (19), the error dynamics on the sliding surface becomes

$$\dot{\tilde{x}} = (I - K(CK)^{-1}C)\Delta f. \tag{31}$$

For our model, since $\tilde{x}_2 = \tilde{x}_3 = 0$, Eq. (31) becomes as follows:

$$\dot{\tilde{x}}_1 = \Delta f_1 - \frac{k_{11}}{k_{21}}\Delta f_2 - \frac{k_{12}}{k_{32}}\Delta f_3 \tag{32}$$

Modelling error $\Delta f(\tilde{x}, t)$ cannot be determined exactly since no information on $f(x, t)$ is available. Here, with the assumption that the friction coefficient is known, the uncertainty is approximated using the vehicle model with the Dugoff's tire model (Dugoff et al., 1970). For a straight driving, where slip angle α is zero and

$$\frac{\mu F_z(1 - \varepsilon_r V_x\sqrt{\lambda^2 + \tan^2\alpha})(1-\lambda)}{2\sqrt{C_i^2\lambda^2 + C_\alpha^2 \tan^2\alpha}} < 1,$$

the tractive force at the tire is expressed by

$$\begin{aligned}F_{xi} &= \mu F_z + \varepsilon_r \mu F_z R\omega_i - \varepsilon_r \mu F_z V_x + \frac{\varepsilon_r \mu^2 F_z^2 R\omega_i}{2C_i} \\ &- \frac{\varepsilon_r^2 \mu^2 F_z^2 R\omega_i V_x}{4C_i} + \frac{\varepsilon_r^2 \mu^2 F_z^2 R^2 \omega_i^2}{4C_i} \\ &- \frac{\mu^2 F_z^2 R\omega_i}{4C_i(V_x - R\omega_i)} \quad (i = f \text{ or } r).\end{aligned} \tag{33}$$

In Eq. (33), only the last term is nonlinear with respect to $V_x (= x_1)$. However, since the last term is smaller than the linear terms, it can be neglected such that tractive forces at front and rear wheels can be expressed respectively by

$$\begin{aligned}F_{xf} &= A_f(\omega_f) + B_f(\omega_f) V_x \\ F_{xr} &= A_r(\omega_r) + B_r(\omega_r) V_x.\end{aligned}$$

Moreover, under the assumption of

$$\Delta f(\tilde{x}, t) := f(\hat{x}, t) - \hat{f}(x, t) \approx \hat{f}(\hat{x}, t) - \hat{f}(x, t) \tag{34}$$

$$\Delta f_1 = \frac{1}{M}(B_f(\omega_f) + B_r(\omega_r))\tilde{x}_1 \tag{35}$$

$$\Delta f_2 = -\frac{R}{I_{wf}} B_f(\omega_f)\tilde{x}_1 \tag{36}$$

$$\Delta f_3 = -\frac{R}{I_{wr}} B_r(\omega_r)\tilde{x}_1. \tag{37}$$

Using above relations, Eq. (32) becomes

$$\dot{\tilde{x}}_1 = c\tilde{x}_1, \tag{38}$$

where

$$\begin{aligned}c &= \frac{1}{M}(B_f(\omega_f) + B_r(\omega_r)) \\ &+ \frac{k_{11}}{k_{21}}\frac{R}{I_{wf}} B_f(\omega_f) + \frac{k_{12}}{k_{32}}\frac{R}{I_{wr}} B_r(\omega_r).\end{aligned} \tag{39}$$

Gains k_{11} and k_{12} are selected appropriately such that c is negative, and thus the error in the vehicle

velocity converges to zero.

5. Simulations

The effects of the designed sliding-mode observer and fuzzy-logic controller are verified by the following simulations. The plant for the simulations is the 14-DOF vehicle model which has nonlinear tire model and the air-brake model. The vehicle parameters of an urban bus (BS-106) are used in the simulations. The simulations are performed for the braking of the straightforward driving vehicle on the slippery road and pressure applied by a driver is 8 bar.

In the first simulation, brake action is triggered when the vehicle is driven on a dry road at 60 km/h. Figure 6 shows the results of the simulation with the sliding-mode observer to estimate the vehicle velocity and wheel speeds. The proposed sliding-mode observer gives satisfactory results for this application of the vehicle ABS control. Vehicle braking characteristics are shown in Fig. 7. Brake pressure fluctuates when vehicle slows down at about 20 to 7 km/h. The slip ratio is about 0.2 most of the period of braking; however, it becomes jumpier as the vehicle approaches near zero due to the fact that it is very sensitive to the wheel speed at such a low vehicle speed. The figure also compares the performance of the system with the PWM control and on-off control under the identical simulation conditions. With the on-off control used, the brake pressure fluctuates vigorously and the controlled slip ratio excessively oscillates around 0.2. Note that even the vehicle speed is a bit more jerky with the on-off control. Thus, it can be concluded the PWM control exhibits a better performance.

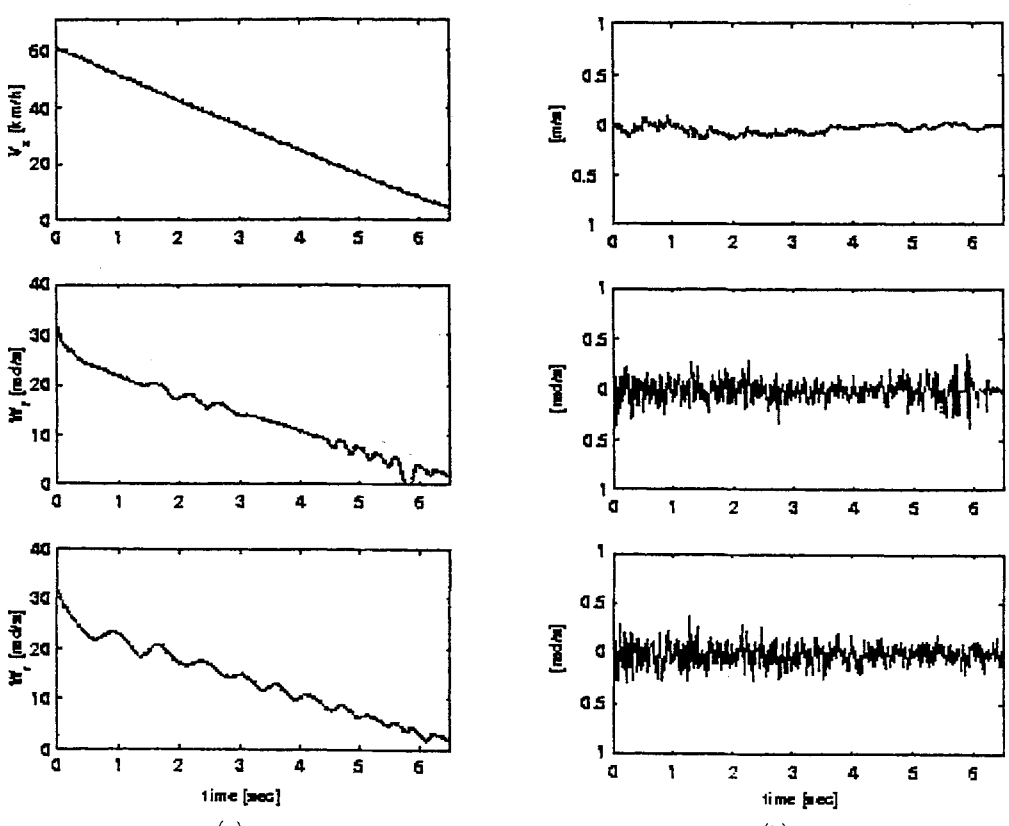

(a) (b)

Fig. 6 (a) Various actual speeds (solid line) and their estimates with the sliding mode observer (dotted line) : vehicle speed, front wheel speed, and rear wheel speed : (b) their estimation errors

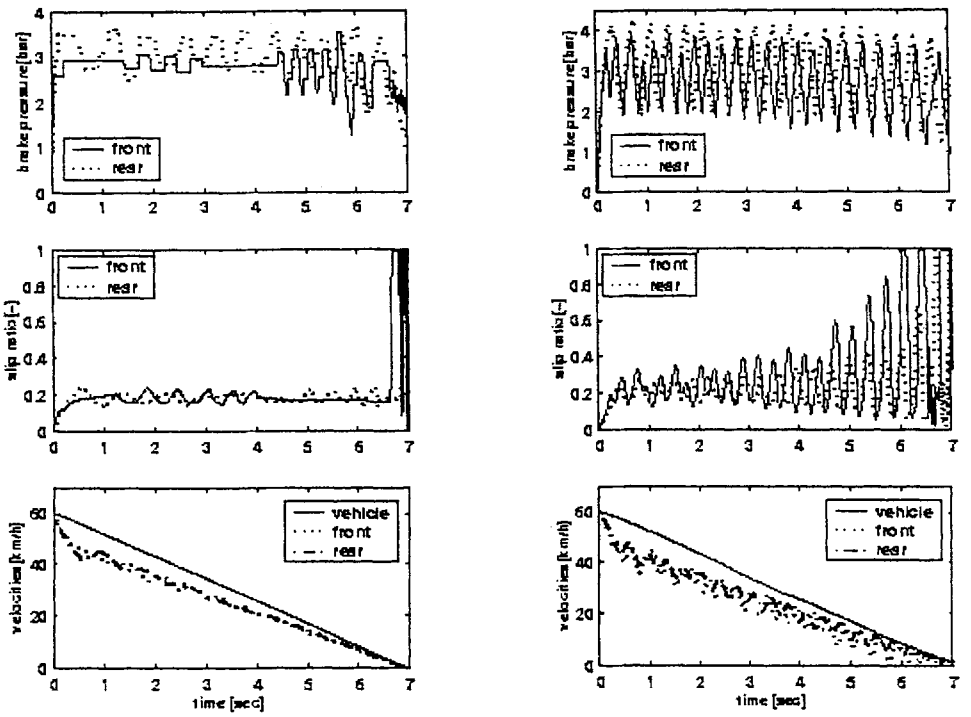

Fig. 7 Vehicle characteristics on a slippery road at 60 km/h with (a) the PWM control inputs, and (b) the on-off control inputs

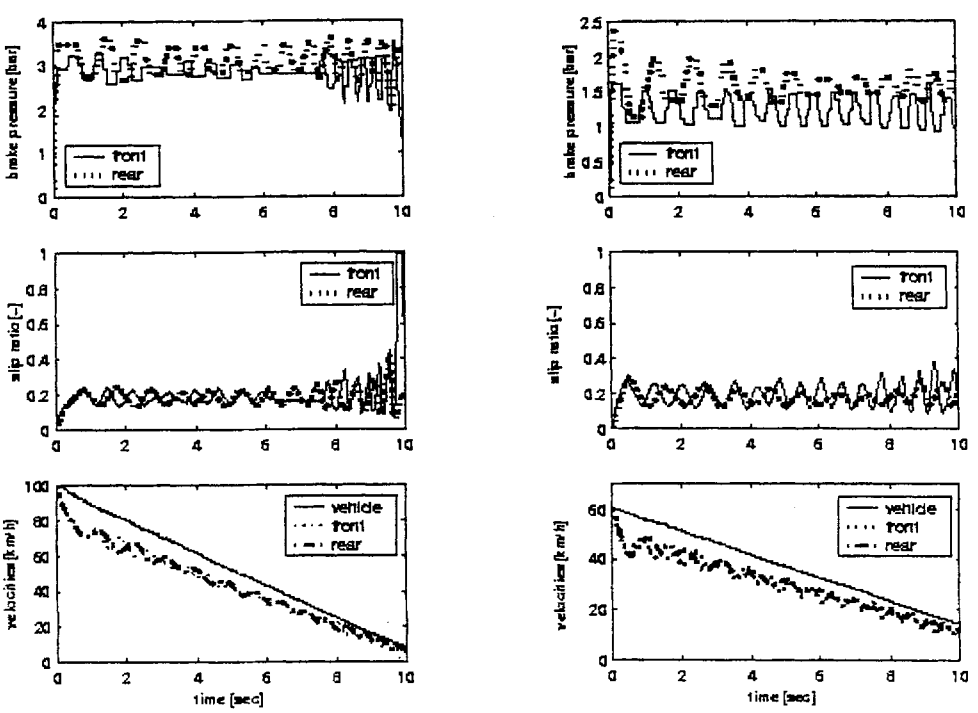

Fig. 8 Vehicle characteristics (a) at higher velocity (100km/h) (b) with lower road friction of μ=0.15

The control performance of the designed fuzzy -logic controller with PWM output is verified via third simulations. Figure 8 shows the results of the simulation. In case (a), only the difference from the first simulation is that the vehicle speed at the moment of initial brake action triggered is 100 km/h instead of 60 km/h. The figure shows that the ABS system performs well in the higher speed. In case (b), the only difference from the first simulation is that the vehicle is driven on a very slippery road (μ=0.15). Even though the slip ratio swings slightly more on the slippery road than on the dry road, the ABS system works well. The figure also shows that it takes more time for the vehicle to stop when it is driven on the slippery road at 60 km/h than when it is driven on the dry road at 100 km/h.

6. Conclusions

An ABS control algorithm for commercial buses is developed based on fuzzy logic. A sliding -mode observer is used to estimate the vehicle speed with the measured wheel angular speed based on a simple 3-DOF vehicle model. The fuzzy-logic controller uses the wheel acceleration and the slip ratio, for which the estimate on vehicle speed with the observer is used. It generates the PWM control input to the pressure control valve. The effectiveness of the proposed control and the observer is confirmed by computer simulations with a nonlinear 14-DOF vehicle model including the nonlinear tire model, and the dynamics model of its brake system. The designed ABS controller is to be implemented and tested in a HILS(hardware-in-the-loop system).

Acknowledgement

This work is supported by Dual-Use Technology Project.

References

Kawabe, T. Nakazawa, M. Notsu, I. and Watanabe, Y., 1997, "A Sliding Mode Controller for Wheel Slip Ratio Control System," *Vehicle System Dynamics*, Vol. 27, pp. 393~408,

Hattori, Y., Takahashi, T. and Tanaka, A., 1998, "An Application of the Adaptive Method for the Sliding Mode Control of the Brake System," *Proc. of AVEC'98*, Vol. 2, pp. 611~619.

Akey, M., 1995, "Development of Fuzzy Logic ABS Control for Commercial Trucks," *SAE 952673*.

Raza, H., Xu, Z., Yang, B. and Ioannou, P. A., 1997, "Modeling and Control Design for a Computer-Controlled Brake System," *IEEE Trans. on Control Systems Technology*, Vol. 5, No. 3, pp. 279~296.

Zanten, A. T. V., Erhardt, R., Pfã, G., Kost, F., Hartmann, U. and Ehret, T. 1996, "Control Aspects of the Bosch-VDC," *Proc. of AVEC'96*, Vol. 1, pp. 573~607.

Watanabe, K., and Kobayashi, K., 1989, "Absolute Speed Measurement of Automobile from Noisy Acceleration and Erroneous Wheel Speed Information," *SAE 982746*.

Choi, S. H. and Cho, D. W., 1998, "Control of Wheel Slip Ratio Using Sliding Mode Controller with Pulse Width Modulation," *Proc. of AVEC' 98*, Vol. 2, pp. 629~635.

Unsal, C. and Kachroo, P., 1999, "Sliding Mode Measurement Feedback Control for Antilock Braking Systems," *IEEE Trans. on Control Systems Technology*, Vol. 7, No. 2, pp. 271~281.

Zimmer, C., 1996, "Fuzzy Approach for Real Time Longitudinal Velocity Estimation of a Road Vehicle in Critical Situation," *Proc. of AVEC'96*, Vol. 2, pp. 1393~1400.

Burke, R. J., Robertson, J. D., Sayers, M. W., and Pottinger, M. G., 1989, "Example Utilization of Truck Tire Characteristics Data in Vehicle Dynamics Simulations," *SAE 982746*.

Slotine, J. J. E. Hedrick, J. K. and Misawa, E. A., 1987, "On Sliding Observers for Nonlinear Systems," *ASME Journal of Dynamic Systems, Measurement, and Control*, Vol. 109, pp. 245 ~252.

Misawa, E. A. and Hedrick, J. K., 1989, "Nonlinear Observers-A State-of-the-Art Survey," *ASME Journal of Dynamic Systems, Measurement, and Control*, Vol. 111, pp. 344

~352.

Dugoff, H., Francher, P. S. and Segel, L., 1970, "An Analysis of Tire Traction Properties and Their Influence on Vehicle Dynamic Performance," *SAE 700377*.

Lin, C. T. and Lee, C. S. G., 1996, *Neural Fuzzy Systems*, Prentice-Hall, Inc.